forests

MDPI

Article

Contrasting Patterns of Tree Growth of Mediterranean Pine Species in the Iberian Peninsula

Edurne Martínez del Castillo [1,2,*], Ernesto Tejedor [1,2], Roberto Serrano-Notivoli [1,2], Klemen Novak [1,2,3], Miguel Ángel Saz [1,2], Luis Alberto Longares [1,2] and Martin de Luis [1,2]

1 Department of Geography and Regional Planning, University of Zaragoza, 50009 Zaragoza, Spain; etejedor@unizar.es (E.T.); rs@unizar.es (R.S.-N.); kn4@alu.ua.es (K.N.); masaz@unizar.es (M.Á.S.); lalongar@unizar.es (L.A.L.); mdla@unizar.es (M.d.L.)
2 Environmental Sciences Institute (IUCA), University of Zaragoza, 50009 Zaragoza, Spain
3 Department of Ecology, University of Alicante, 03690 Alicante, Spain
* Correspondence: edurne@unizar.es

Received: 6 June 2018; Accepted: 10 July 2018; Published: 11 July 2018

Abstract: Wood formation is the primary biological process through which carbon is durably sequestered in woody plants, and is thus a major contributor to mitigate climate change. We analyzed the tree growth patterns of four conifer species across the Iberian Peninsula (IP) based on a dense dendrochronological network (179 sites) combined with a high resolution climate dataset. Generalized linear-mixed models were used to predict the potential tree growth of different pine species under different climate conditions considering different age classes. We found a strong age dependency of tree growth, significant variations across the climate gradients, and a significant interaction of both age and climate effects on the four species considered. Overall, *Pinus halepensis* was the species with the highest climate sensitivity and the highest growth rates in all age classes and across its distribution area. Due to its stronger plastic character and its potential adaptability, *Pinus halepensis* was demonstrated to be the most suitable species in terms of tree growth and potentiality to enhance carbon sequestration in the IP. Since its potential distribution largely exceeds its actual distribution, *P. halepensis* arises as a key species to cope with future climate conditions and to keep fixing carbon regardless of the climatic circumstances.

Keywords: tree-rings; dendrochronology; basal area increment; Generalized Linear Mixed-Effects models; *Pinus halepensis*; *Pinus sylvestris*; *Pinus uncinata*; *Pinus nigra*; climate; age-effects

1. Introduction

Forests world-wide are known as major biotic long-term storage for carbon and therefore play an important role in the global carbon cycle. Biomass formation is the primary biological process through which carbon is sequestered by plants via photosynthesis. Specifically, wood formation is the main contributor to the global net of the forest carbon sink of about 2.5 petagrams of carbon per year [1]. As the forest grows and produces wood, around 15% of the anthropogenic carbon dioxide (CO_2) emissions are absorbed in the process, helping to mitigate climate change [1–3]. However, the patterns of terrestrial carbon exchange may already be changing as a consequence of land-cover and use modifications and large-scale environmental changes [4]. Higher rates of forest growth and enhanced wood production are projected to occur in northern boreal and temperate zones due to increasing temperatures and CO_2 and nitrogen fertilization [5–7]. Contrarily, predictions forecast a decrease in forest productivity over Mediterranean climates, because the tree growth enhancement produced by fertilization is not expected to compensate for the possible constrains resulting from changes in temperature and rainfall [8]. Despite recent advances, large uncertainties and knowledge

gaps remain in the response of the global carbon cycle to continuing climate change [9] and the exact estimation of forest productivity is currently hampered by our limited understanding of the climatic drivers of wood formation as a function of species, ecological conditions, and geographic location [10].

Tree secondary growth as annual basal area increments represents a direct proxy for forest ecosystem performance, and can be derived from dendrochronological records [11]. Growth measurements obtained from increment cores are tightly linked with stem productivity and with the stand-level net primary growth, and their analysis provides key information for understanding the carbon-location within trees [12]. In addition, tree secondary growth data is shown to be broadly compatible with productivity estimations from forest inventory data [13], eddy-covariance measurements [14], and carbon budget models [15]. Moreover, dendroclimatological studies provide insights on the actual influence of environmental constraints on tree biomass, the species-specific influence of climate drivers in tree growth, and how such influences can vary during their life trajectory [16]. Furthermore, the establishment of regional-scale networks allowed the spatial and species-specific growth response patterns to be connected with thermal and moisture variations within particular climatic zones [17–23].

In this regard, numerous dendroclimatological studies have provided new insights on the influence of climate variability on different forest species across the Mediterranean area, particularly in the Iberian Peninsula [24–29]. Species-specific climatic drivers have been identified and their influence has been quantified. Also, the geographical variations in climate influences have been highlighted [23,30–32]. However, tree-ring chronology classical procedures include standardizations to remove biological trends and non-climate signals in tree-ring measurements by transforming growth width into growth indices [33–35]. As a consequence, despite the fact that the patterns of growth are well known to vary over the life span of trees, a detailed quantification of how aging effects growth and how this differs between species or across the geographical range of the distribution of species is rare in dendrochronological studies [16,36]. Similarly, growth magnitude is removed from tree-ring series by the detrending process and so studies focused on comparisons of growth rates between species or variations in growth rates across environmental gradients are also rare.

Here, we perform an Iberian peninsula-wide analysis of tree growth patterns based on an extensive dendrochronological network of 179 tree stands of four key coniferous species. The sampling points are spread along the complete climatic gradients present on the different species distribution, including a wide range of age classes. The dendrochronological network is combined with a high resolution climate dataset [37,38] to assess (1) how tree-growth and the influence of the climate drivers vary with tree age; (2) how climate-growth relationships vary across species' distribution; and (3) how growth and climate influence (and its variations) differ between species. The final aim is to successfully quantify the nature of those effects (i.e., age, climatic gradient, and species) on tree growth to improve the knowledge on their potential impact on forest productivity.

2. Methods

2.1. Study Area and Dendroclimatic Dataset

The study region essentially comprises the Mediterranean climate region of the Iberian Peninsula where we sampled and compiled raw tree-ring width information from a total of 179 study sites (Figure 1) of four different Pinaceae species (*Pinus halepensis* Mill., *Pinus sylvestris* L., *Pinus uncinata* Ram., and *Pinus nigra* Arnold.). Over all the study sites, 39 were free-access sites downloaded from The International Tree-Ring Data Bank (ITRDB), 19 came from the Spanish National Research Council (CSIC) and the University of Zaragoza, and the rest (i.e., 121) were sampled by the University of Zaragoza. Altogether, the tree-rings of 2982 trees and 5637 cores have been analyzed. A catalogue of 179 sites is available in Table S1.

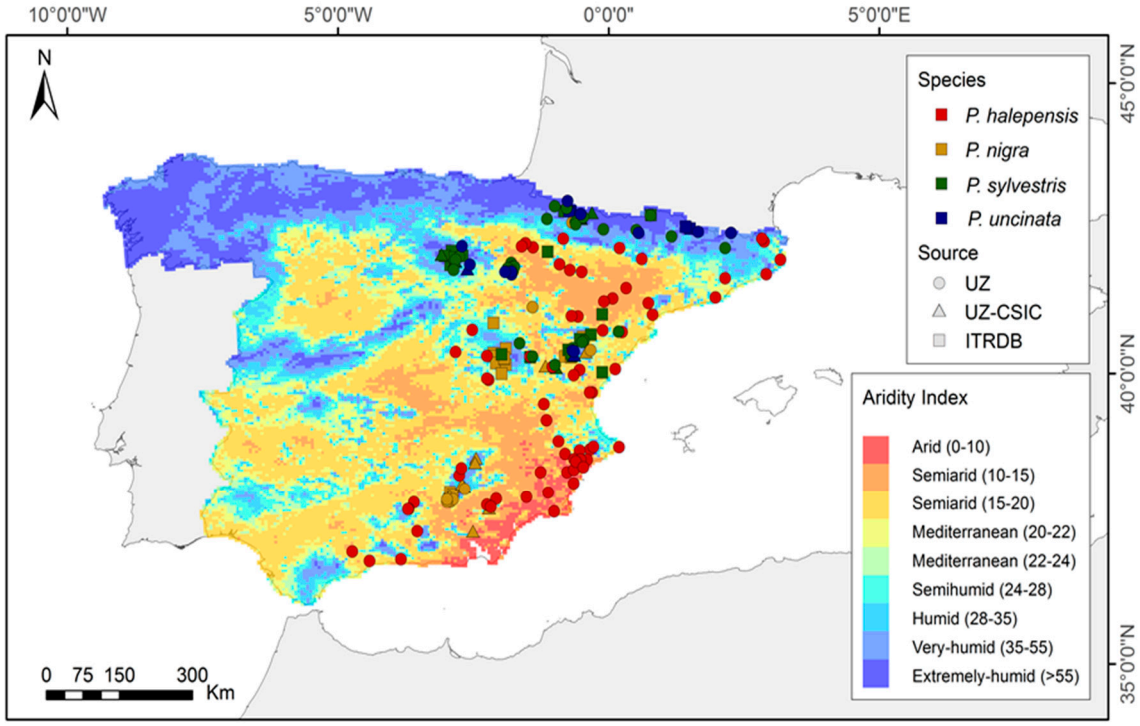

Figure 1. Sampling points location map.

At each site sampled by the University of Zaragoza, five to 88 mature, healthy, and dominant trees were selected and cored at breast height (1.3 m) between 2000 and 2016. The range of altitudes covered by the sampling ranged from 1 m a.s.l. (in the case of *Pinus halepensis* growing close to Mediterranean shore) to 2100 m a.s.l. (in the case of *Pinus uncinata* sampling point in the Pyrenees). Trees were cored from two to three times each using Pressler increment borers. The cores were air-dried, mounted on wooden supports, and sanded to obtain a radial section. Later, the cores were scanned and cross-dated using CooRecorder v8.0 software (Cybis Elektronik & Data AB. Saltsjöbaden, Sweden) [39] and verified using COFECHA software [33]. The tree-ring width measurement was done to the nearest 0.01 mm with the TSAP-Win program and a LINTAB™ 5 measuring device (Rinntech, Heidelberg, Germany).

In the case of cores were the pith was reached, the cambial age at breast height of each individual tree-ring was directly calculated from counts of the annual growth rings in the sample. In cores without pith or those measurements obtained from external sources, the pith-offset estimations were calculated by fitting a geometric pith locator to the innermost ring [40]. Then, after calculating the missing rings to the pith, the cambial age was estimated by adding the counted tree-rings in the oldest sample of the tree and the estimated missing rings. Then, the tree-ring width series were converted into basal area increment (BAI), which accounts for the geometrical constraint of adding a volume of wood to a stem of an increasing radius [41]. Locally absent tree-rings in the cores were previously assigned to have a width of 1/100 mm. The BAI series for each tree was obtained by using the formula:

$$BAI_{t,y} = \pi\left(r_{t,y}^2 - r_{t,y-1}^2\right) \quad (1)$$

where $r_{t,y}$ and $r_{t,y-1}$ are the stem radii corresponding to the tree t for years y and $y-1$, respectively. Finally, a mean BAI series for each individual tree was calculated by averaging BAI series of the cores corresponding to each tree.

The monthly mean temperature and total monthly precipitation from the closest gridpoint to each forest site were obtained from the high resolution SPREAD (Spanish PREcipitation At Daily scale) climate dataset [37]. Annual precipitation and mean annual temperature, calculated from the

previous September to the current August, were calculated for each site and year to describe the climate conditions which occurred during the year of each tree-ring formation. Since SPREAD spans from 1950 to 2014, the dendroclimatic dataset was limited to the common period.

In order to highlight the most distinct climate gradient across the study area, mean annual temperature and total annual precipitation were combined into a single simple parameter representing a measure of the precipitation effectiveness. We used the aridity index (AI) proposed by De Martonne (1926) [42], which is calculated by using the formula:

$$AI_{s,y} = \frac{P_{s,y}}{10 + T_{s,y}} \quad (2)$$

where $P_{s,y}$ is the total precipitation (in mm) which occurred in site s in the year y and $T_{s,y}$ is the mean annual temperature (in °C) which occurred in site s in the year y. Climate types defined by AI ranges from arid (0–10) to semi-arid (10–20), Mediterranean (20–24), semi-humid (24–28), humid (28–35), very humid (35–55), and extremely humid (>55).

2.2. Analyzed Variables

For the study period 1950–2014, a total of 147,337 tree-rings were used. The age structure of analyzed tree-rings is shown in Figure 2b. For all four analyzed species, the juvenile phase of tree growth was well represented in the dendroclimatological dataset. The cambial age of the tree-rings of *P. halepensis* (PIHA) ranged from 1 to 215, with a median of 42 years. The oldest tree-rings for *P. sylvestris* (PISY), *P. uncinata* (PIUN), and *P. nigra* (PINI) are 505, 528, and 939 years, with a median of 82, 124, and 220 years, respectively.

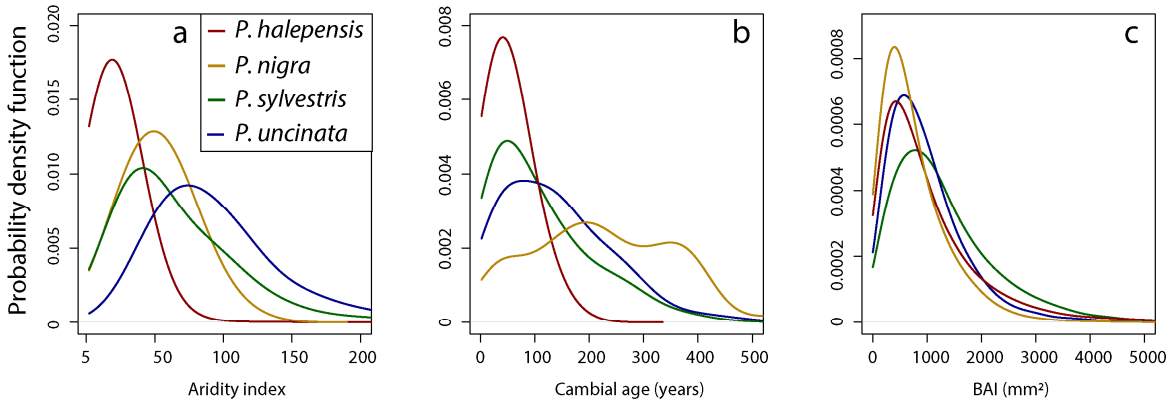

Figure 2. Density distribution of tree-rings with regards to (**a**) their distribution in different aridity conditions, (**b**) their cambial age, and (**c**) the basal area increment that they represent.

Density profiles were calculated using the density generic function in R computing environment, which computes kernel density estimates. Globally, the climate range represented in the dendroclimatic dataset largely included all climate types defined by the aridity index (Figure 2a). PIHA populations are located in the more xeric sites of the study area, where mean annual precipitation can be lower than 210 mm, and in extremely dry years, even lower than 60 mm. Mean annual temperatures can be, in contrast, higher than 18.2 °C, with extremely warm years that can reach 19.6 °C. Consequently, PIHA tree-rings included in our dataset have, on average, lower AI values (median of 18.11) compared with other studied species (i.e., 50.2 for PINI, 51.8 for PISY, and 85.0 for PIUN). In the case of PIHA, tree rings formed under arid conditions (AI < 10) are well represented in our dataset (n = 7599), including nearly all age classes of the species (tree-rings from one to 211 years old). The presence of PIHA tree-rings with well represented age classes extended up to extremely humid conditions (of AI up to 86). The presence of tree-rings that formed under arid conditions is much lower in the other

pine species (PISY: n = 325; PINI: n = 228; PIUN: n = 0) including, in addition, a limited number of age classes. A representative number of tree-rings of PISY span from semiarid conditions (AI = 10) to extremely humid conditions, (AI = 142), while tree-rings of PINI and PIUN are restricted to the Mediterranean AI climate type (AI > 20 in PINI and AI > 22 in PIUN), but also reach the extremely humid type climate (AI = 122 in PINI and AI up to 299 in PIUN).

Individual tree annual basal area increments, as recorded in the dendroclimatic dataset, have been used as the primary variable of interest for the tests identifying differences among species and to test for the effect of tree age and the aridity gradient in tree growth. BAI shows a skewness distribution in all four species analyzed. The median annual BAI in the tree-rings included in the dataset are 753, 1086, 999, and 589 mm^2 for PIUN, PISY, PIHA, and PINI, respectively. Density profiles of the BAI of each species are shown in Figure 2c.

2.3. Statistical Procedures

Generalized linear-mixed models were used to evaluate the effect of tree-age (AGE) and aridity gradient on BAI and their differential effects on studied species (SPECIES). The annual BAI value was used as a dependent variable and their corresponding SPECIES, AI, and AGE values as predictors (fixed factors). The interaction between them was also considered in the models. Since both dependent and independent variables have a skewed distribution, all variables have been logarithmically transformed before model computation. Then, log transformed AGE and AI were standardized to have a zero mean and a standard deviation of one to ensure that the predictors used will be on the same scales. In addition, since BAI represents repeated measures over the same individuals, tree identity was also included in the models as a random factor. Analyses were performed in R environment and the lme4 package was used to produce Generalized Linear Mixed-Effect models [43]. Since Log (BAI) cannot obtain negative values, the model was constructed using the Poisson family to describe the error distribution. Then, a final full model was constructed according to the equations (formula in R language).

$$\text{glmer}(\log(\text{BAI}) \sim \text{SPECIES} * \log(\text{AI})_{std} * \log(\text{AGE})_{std} * (1|TREE), \quad (3)$$

$$family = poisson(link = \text{“log”})$$

The accuracy of the model was evaluated using a likelihood ratio test by comparing the obtained model (full model) with a set of restricted models where the explanatory variables of interest are sequentially omitted (leave-one-out validation analysis) until it only includes the intercept term (null model). The p-value of the likelihood ratio test that compares the full and reduced models was calculated using the chi-square test and its related probability level (P) [44]. In addition, the explained variance (r^2) of each model was also computed.

Then, the model with the better performance was selected and applied to obtain BAI predictions for a theoretical tree across the matrix-range of AI and AGE values where each species is present in the original dataset (Figure 3). Finally, the predicted cumulative BAI was calculated for a theoretical tree from age one to age 100 years growing in the different climate type AI classes as a general overview of species performance.

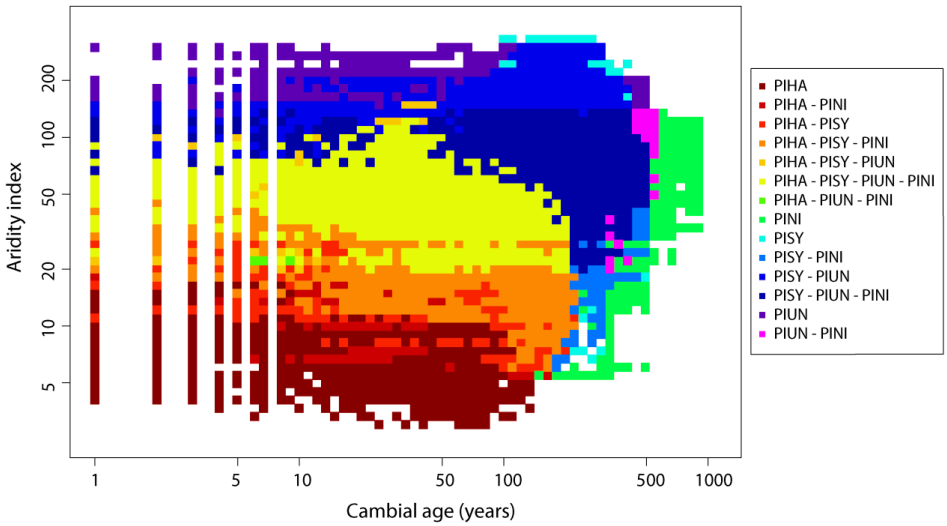

Figure 3. Matrix range of aridity gradient and age (AI-AGE) describing the space where species are present and/or coexist.

3. Results

3.1. Accuracy of Predictive Models

Generalized mixed models constructed to predict BAI using AGE, AI, and SPECIES as fixed factors were strongly significant, and all three factors included and the interactions between them were also significant (Table 1). The performance of full models significantly differed from null models, showing lower AIC (Akaike information criterion) weight and significantly higher explained variance.

Table 1. Accuracy assessment of the models. Parameters: Df (number of parameters in the model), AIC (Akaike information criterion), BIC or SBC (Schwarz's Bayesian criterion), logLiK (log-likelihood function), Chisq (Chi-squared test), Chi_Df (Chi-squared degrees of fredom), and Pr(>Chisq) (significance level).

	Df	AIC	BIC	LogLik	Deviance	Chisq	Chi_Df	Pr(>Chisq)
AI*AGE model	5	5,543,529	5,543,579	−2,771,760	5,543,519			
SPECIES*AI*AGE	17	5,298,138	5,298,307	−2,649,052	5,298,104	245,415	12	$<2 \times 10^{-16}$
Null model	2	6,361,579	6,361,598	−3,180,787	6,361,575			
SPECIES*AI*AGE	17	5,298,138	5,298,307	−2,649,052	5,298,104	1,063,470	15	$<2 \times 10^{-16}$

Parameters of the final models obtained for each species are shown in Table 2. The observed and the predicted values for BAI according to these models, including the explained variance (r^2) in each case, are shown in Figure 4.

Table 2. Parameters of Basal Area Index models of the analyzed species. AI, AGE, and AI:AGE (interaction between the aridity index and the tree age).

		Estimate	Std. Error	z Value	Pr(>|z|)
PISY	(Intercept)	9.68e+00	1.69e-03	5718	<2e-16
	AI	1.04e-02	1.04e-04	101	<2e-16
	AGE	3.54e-02	1.06e-04	335	<2e-16
	AI:AGE	4.22e-03	9.48e-05	45	<2e-16
PIUN	(Intercept)	9.65e+00	2.68e-03	3595	<2e-16
	AI	4.97e-03	1.48e-04	34	<2e-16

Table 2. *Cont.*

		Estimate	Std. Error	z Value	Pr(>|z|)
	AGE	4.87e-02	2.41e-04	202	<2e-16
	AI:AGE	7.12e-03	1.45e-04	49	<2e-16
PIHA	(Intercept)	9.74e+00	1.64e-03	5945	<2e-16
	AI	6.04e-02	9.47e-05	638	<2e-16
	AGE	5.12e-02	9.43e-05	543	<2e-16
	AI*AGE	1.71e-02	8.41e-05	203	<2e-16
PINI	(Intercept)	9.60e+00	2.64e-03	3640	<2e-16
	AI	3.49e-03	1.63e-04	21	<2e-16
	AGE	6.15e-02	2.14e-04	287	<2e-16
	AI:AGE	7.69e-04	1.40e-04	6	3.79e-08

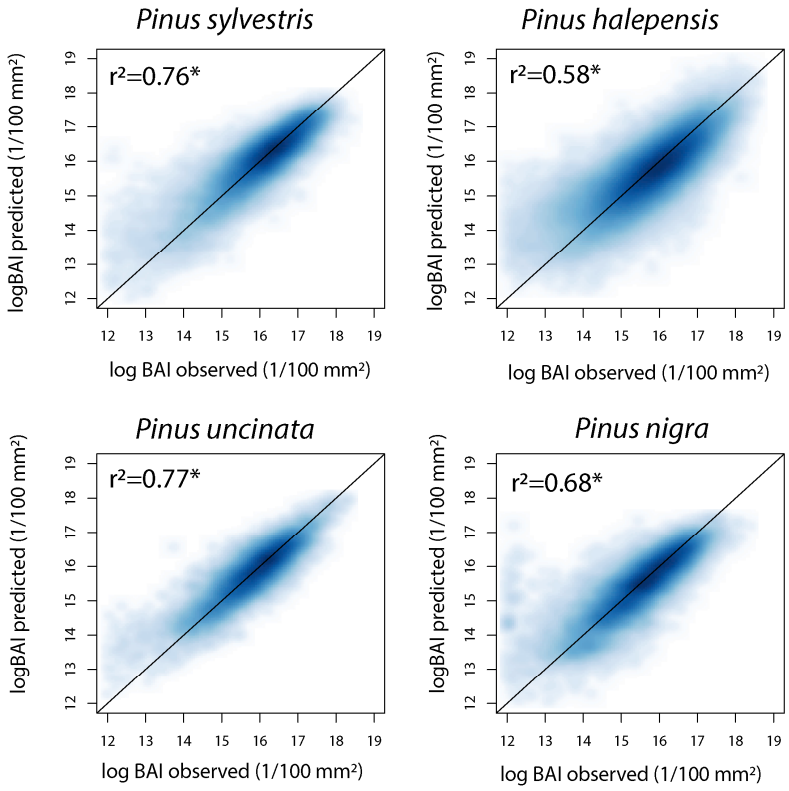

Figure 4. Basal Area Index predicted (log) using the Generalized Linear Mixed-Effects models versus the observed BAI (log). The explained variance of the models (r^2) is shown. The asterisk indicates a significance level $p < 0.001$.

The analysis confirms a strong dependency effect of the annual BAI of the four species in relation to AGE and also strong and significant variations across the aridity gradient (Table 2). Altogether, variations in AI and AGE are able to explain 58% of the total variance in BAI in the case of PIHA and 68%, 76%, and 77% in the case of PINI, PISY, and PIUN, respectively (Figure 4a–d).

3.2. Age Effect on BAI Performance and Differences Along AI Gradient

In all four species, annual BAI significantly increases as trees became older and as aridity conditions decrease (higher AI values). The interaction between these two factors is, in addition, significant in all four species, suggesting that the AGE effects differ across the aridity gradient (see

models estimates in Table 2). Patterns of variation of BAI for all existing age classes and AI conditions of each species are shown in Figure 5.

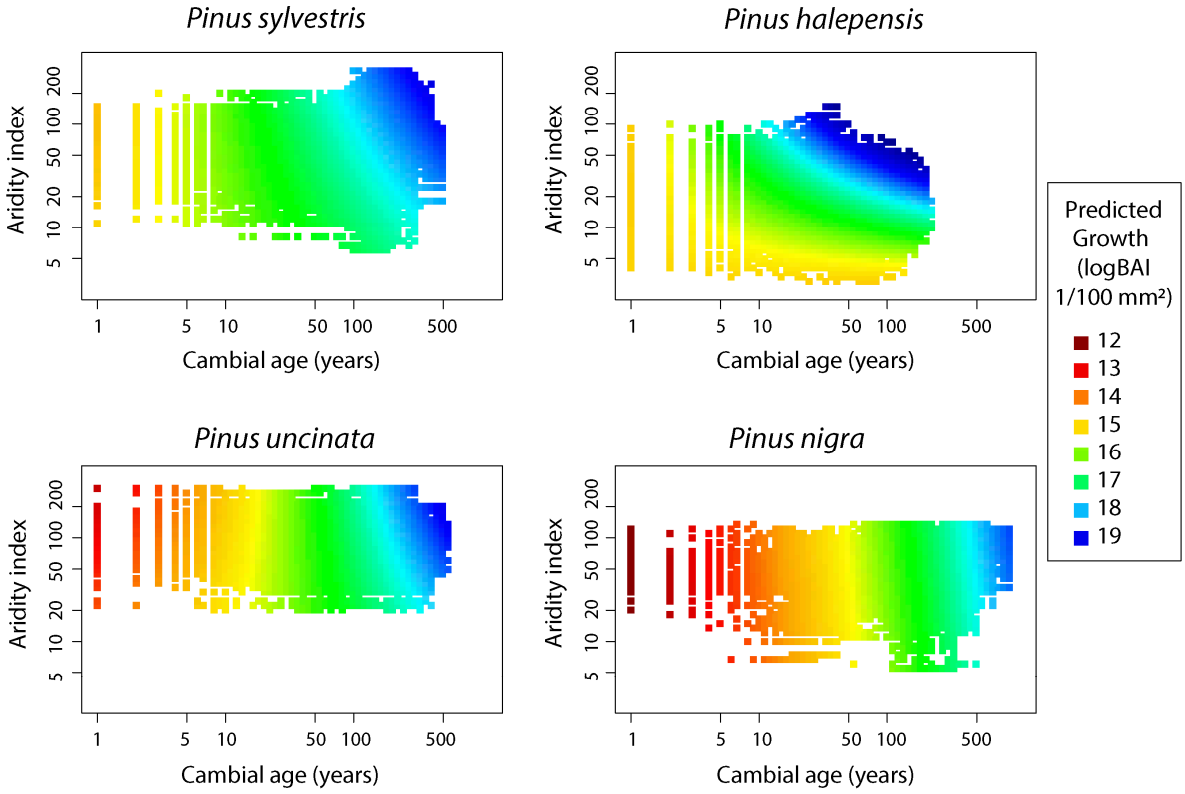

Figure 5. Predicted growth (in log BAI 1/100 mm^2) over different climate conditions and tree ages where the species are present.

In general, the lower predicted BAI values are observed for juvenile PINI trees with values even lower than 0.14 cm^2/year. Low annual growth rates (<0.25 cm^2/year) are also described for juvenile PIUN trees, especially those growing under humid conditions (high AI). In PISY, lower growth rates are also observed during the juvenile phase, but growth is higher than in the previous species, with BAI always being higher than 1 cm^2/year. In the case of PIHA, juvenile trees and mature ones growing at arid conditions (AI < 10) exhibit lower annual growth rates, but these were always higher than 1.1 cm^2/year. Contrarily, higher growth rates are observed in mature trees of PIHA growing under very humid and extremely humid conditions (AI > 35), where BAI can reach values even higher than 75 cm^2/year. PISY and PIUN reach a maximum BAI of around 35 cm^2/year, but this is also restricted to extremely humid conditions and older trees (higher than 200 years old). The maximum growth rate of PINI is the lowest observed in all four species, with a BAI of 24.4 cm^2/year also described for extremely humid conditions and very old trees (>500 years old) (Figure 5a–d).

3.3. Differences between Species' BAI

Model predictions allow direct comparisons of BAI of all analyzed species under equivalent age classes and climate conditions. The annual mean BAI from the juvenile (one year old) to adult phase (100 years old) averaged by AI climate types existing in the study area allows for a summary of species behavior in relation to their growth rates and, therefore, their efficiency in the use of water (Figure 6).

Several clear findings emerged from this analysis. The presence of PIHA extended from arid (AI < 10) to extremely humid climate types (AI > 55). Across this wide range of conditions, PIHA is the species with higher growth rates and a higher sensitivity to AI variations. On the other extreme, PINI is the species with the lowest growth rates and the lowest variations across the AI climate

type classes where it is present. The BAI of PISY is just slightly lower than that of PIHA in xeric conditions, but differences between species increase in favor of PIHA as aridity decreases. PIUN exhibits an intermediate behavior, showing higher BAI than PINI but lower than PISY in all climate type classes.

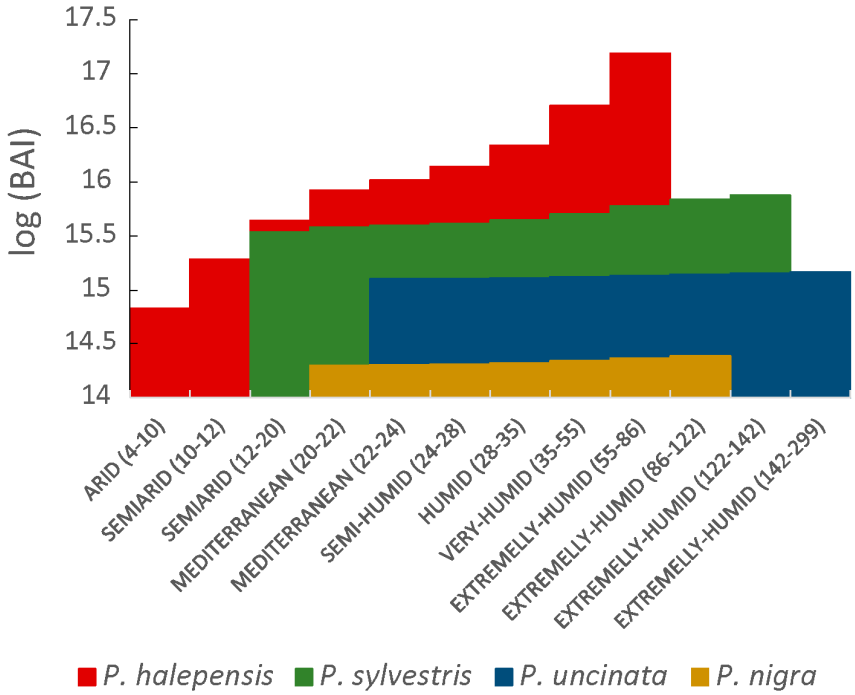

Figure 6. Estimated log BAI gain (in 1/100 mm^2) of a hypothetical 100 years old tree over all climate conditions where the species are present for all species.

4. Discussion

4.1. Age Effects on Carbon Uptake

The Mediterranean forest has suffered continuous changes in its distribution throughout the past millennia, mainly due to the combined action of human activities on the landscape and as the effects of the recent warming and droughts increase [45]. Although forest cover has increased during the last decades in Mediterranean areas, the changes suffered are related to a reduction in forest health and productivity [1,45].

The capacity to resist drought by long-term adaptation and evolution in drought environments is a demonstrated characteristic of Mediterranean species that can contribute to their persistence under projected increases of drought in the Mediterranean regions of the Iberian Peninsula [45]. Heterogeneous responses of species to climate variability across their range are directly connected to the phenomena of local adaptation and phenotypic plasticity and are the basis of potential adaptability to future climate conditions [23]. A detailed knowledge of the relationship between climate and growth during the tree life span and across the range of the distribution of species is then essential to predict and mitigate the effects of climate change [46].

In this context, our results generally showed that the stem basal area increment was initially small, but rapidly increased with tree age. The existence of this growing pattern during the tree life span is well-known in scientific literature [47,48], but the results we provided allow, for first time, an exact quantification of the magnitude of the age effect on BAI for four representative conifers in the Mediterranean area of the Iberian Peninsula. Moreover, we found that biological trends in tree growth showed significant variations across species distribution over diverse aridity conditions where

populations are developed. This finding is especially relevant for future growth and carbon sink predictions under climate change scenarios, since aridity conditions are expected to increase in the future, and consequently, biological growth trajectories can be expected to change.

The significant interaction between tree-age and climate drivers recorded in this analysis may be considered as a new challenge in dendroclimatic reconstructions, since it could contribute to solving the divergence problem observed in other latitudes [49]. The detrending methods typically applied in those reconstructions are supported by the assumption of the independency of the age over the climate signals, which disagrees with our findings. Our results are limited to four pine species growing in a specific geographical area, but if such patterns may occur elsewhere, it may have serious implications by affecting the reliability of tree-ring based climate reconstructions. Future efforts need to be done in relation to this, and mixed models could be tested as an alternative detrending tool for dendroclimatological research.

4.2. Future of Forest Growth in the Iberian Peninsula

Irrespective of the aridity conditions, *P. halepensis* was the species with a better growth performance across its distribution range, including the areas shared with the other species analyzed (e.g., in Teruel and Cuenca provinces). This species is traditionally described as a pioneer, opportunistic, and the most drought tolerant conifer species. Therefore, the higher growth rates observed in arid and semiarid conditions do not represent a novelty in scientific literature [50]. However, we found that these higher growth rates are extended and even magnified under humid and extremely humid conditions (i.e., close to the main East ranges of the Iberian Peninsula: the Pyrenees, the Iberian Range, and the Baetic mountains). On the other hand, drought and frosts are the major constrains of plant functioning and distribution in the Mediterranean area, but recent research suggests that limits for *P. halepensis* distribution in juvenile phases are especially related to the frost tolerance of foliage rather than other environmental stresses. In this sense, *P. halepensis* was described as the least frost tolerant species, while *P. sylvestris*, *P. uncinata,* and *P. nigra*, which inhabit the coldest locations, are significantly more frost tolerant species [51]. Controversially, other studies suggest that winter and spring rainfalls are the most important predictor for the main pine species distribution, whereas temperature was a secondary or tertiary factor [52]. Our study suggests that drought, instead of frost, was the key climatic factor explaining variations in growth patterns. However, we also highlight that the influence of different climate stressors significantly differed depending on tree cambial age.

Moreover, the results provided new evidence of pines' high plastic character in terms of growth rhythm adaptations to climate variability. *P. sylvestris*, *P. uncinata,* and specially *P. nigra*, showed lower growth rates than *P. halepensis* across their common distribution areas but, more importantly, they showed lower variations in their growth patterns under their climate distribution range. Several recent studies highlight the substantial phenotypic plasticity of *P. halepensis* in relation to different anatomical, reproductive, and vegetative traits [28,53–58]. As with the majority of species, cambial activity can stop for several months during the winter [59]. Nevertheless, under favorable growing conditions, the vascular cambium may be active throughout the entire year [59,60]. Besides, this species can also adapt to double stress conditions, also ceasing cambial activity during summer (i.e., by high temperatures and lack of precipitation) [61,62] or ceasing secondary tree growth completely during a year with extreme limiting conditions [63].

Forests can play a role in mitigating climate change through the capture and storage of carbon [45]. Appropriate reforestation is the main way to contribute to this challenge and our study suggests that *P. halepensis* can be a suitable species for this purpose, especially aged forests of this species growing in moist environments. Indeed, *P. halepensis* is the most common tree species occupying large areas with harsh environmental conditions where other tree species are not able to survive [50]. However, its potential distribution largely exceeds the actual distribution [52] and is expected to increase in the future [64]. Meanwhile, the suitability of other conifers is expected to decrease [65].

Tree-ring data have been useful in developing stand-level biomass reconstructions to investigate long-term trends in aboveground productivity [66–68]. There are, however, several limitations to using tree-ring records to infer climate sensitivities of carbon uptake [69]. In most tree-ring analyses, and also in our study, the mean basal area increment across different individuals is used to represent growth at the site level. Factors such as competition, topography, and especially stand density are not captured by sampling and only through dominant and codominant individual trees, as is common in dendrochronological studies [69]. Therefore, ecological sampling designs where all individuals in a fixed plot or a random sub-sample are included would need to be considered to estimate forest productivity at a landscape level (e.g., [68,70]).

The evaluation of the sensitivity of carbon uptake to climate, however, is also challenging using alternative approaches. Methods such as forest inventories, eddy-covariance towers, or the use of remote sensing techniques are limited to estimating the carbon uptake of a fraction of the lifespan of trees and in response to the current or recent climate. Furthermore, harmonized continental- or regional-scale estimates often rely on simplifying assumptions, such as the use of global, non-species, or site-specific allometric equations that complicate comparisons with field data [69].

In this paper, we advocated for a tree-centered approach [71] as a complementary method to improve the mechanistic understanding of physiological and growth responses of trees growing under various conditions. This knowledge complements other approaches and can, for instance, support forest managers in tree species and/or provenance selection to better prepare specific forest stands to cope with expected challenges.

5. Conclusions

The patterns of tree growth of the main Mediterranean pine species in the Iberian Peninsula were characterized by a high variability across the territory. The variability found in the tree basal area increment was highly influenced by tree age and climate. Moreover, the interaction of age and climate conditions is a determinant for tree growth, showing a distinct influence between the different species. In this sense, the stronger plastic capacity and the potential adaptability of *P. halepensis* makes it the key species to cope with uncertain climate conditions and to keep fixing carbon regardless of the climatic circumstances.

Supplementary Materials: The following are available online at http://www.mdpi.com/1999-4907/9/7/416/s1.

Author Contributions: Conceptualization was done by E.M.d.C. and M.d.L.; Methodology was done by E.M.d.C., R.S.-N., K.N. and M.d.L.; Analysis was done by E.M.d.C., E.T. and M.d.L. Investigation was done by, E.M.d.C., E.T., R.S.-N., K.N., M.A.S., L.A.L. and M.d.L.; Writing the original draft was done by E.M.d.C. and M.d.L.; Writing—Review and Editing was done by E.M.d.C., E.T., R.S.-N., K.N., M.A.S., L.A.L. and M.d.L.; Project Administration was done by M.A.S.; Funding Acquisition was done by M.d.L., L.A.L. and M.A.S.

Funding: This research was funded by the Spanish "Ministerio de Economía y Competitividad" (MINECO), by the research project CGL2015-69985-R.

Acknowledgments: We were supported by the Government of Aragon through the 'Program of research groups' (group 'Clima, Cambio Global y Sistemas Naturales'). We would like to thank anonymous reviewers for their helpful comments.

Conflicts of Interest: The authors declare no conflict of interest.

References

1. Pan, Y.; Birdsey, R.A.; Fang, J.; Houghton, R.; Kauppi, P.E.; Kurz, W.A.; Phillips, O.L.; Shvidenko, A.; Lewis, S.L.; Canadell, J.G.; et al. A large and persistent carbon sink in the world's forests. *Science* **2011**, *333*, 988–993. [CrossRef] [PubMed]
2. Friedlingstein, P.; Houghton, R.A.; Marland, G.; Hackler, J.; Boden, T.A.; Conway, T.J.; Canadell, J.G.; Raupach, M.R.; Ciais, P.; Le Quéré, C. Update on CO_2 emissions. *Nat. Geosci.* **2010**, *3*, 811–812. [CrossRef]

3. Cuny, H.E.; Rathgeber, C.B.K.; Frank, D.; Fonti, P.; Makinen, H.; Prislan, P.; Rossi, S.; Martínez del Castillo, E.; Campelo, F.; Vavrčík, H.; et al. Woody biomass production lags stem-girth increase by over one month in coniferous forests. *Nat. Plants* **2015**, *1*, 15160. [CrossRef] [PubMed]
4. Schimel, D.S.; House, J.I.; Hibbard, K.A.; Bousquet, P.; Ciais, P.; Peylin, P.; Braswell, B.H.; Apps, M.J.; Baker, D.; Bondeau, A.; et al. Recent patterns and mechanisms of carbon exchange by terrestrial ecosystems. *Nature* **2001**, *414*, 169–172. [CrossRef] [PubMed]
5. Hoch, G.; Körner, C. Global patterns of mobile carbon stores in trees at the high-elevation tree line. *Glob. Ecol. Biogeogr.* **2012**, *21*, 861–871. [CrossRef]
6. Sitch, S.; Huntingford, C.; Gedney, N.; Levy, P.E.; Lomas, M.; Piao, S.L.; Betts, R.; Ciais, P.; Cox, P.; Friedlingstein, P.; et al. Evaluation of the terrestrial carbon cycle, future plant geography and climate-carbon cycle feedbacks using five Dynamic Global Vegetation Models (DGVMs). *Glob. Chang. Biol.* **2008**, *14*, 2015–2039. [CrossRef]
7. Zhao, M.; Running, S.W. Drought-Induced Reduction in Global. *Science* **2010**, *329*, 940–943. [CrossRef] [PubMed]
8. Lindner, M.; Maroschek, M.; Netherer, S.; Kremer, A.; Barbati, A.; Garcia-Gonzalo, J.; Seidl, R.; Delzon, S.; Corona, P.; Kolström, M.; et al. Climate change impacts, adaptive capacity, and vulnerability of European forest ecosystems. *For. Ecol. Manag.* **2010**, *259*, 698–709. [CrossRef]
9. Moss, R.H.; Edmonds, J.A.; Hibbard, K.A.; Manning, M.R.; Rose, S.K.; Van Vuuren, D.P.; Carter, T.R.; Emori, S.; Kainuma, M.; Kram, T.; et al. The next generation of scenarios for climate change research and assessment. *Nature* **2010**, *463*, 747–756. [CrossRef] [PubMed]
10. Stegen, J.C.; Swenson, N.G.; Enquist, B.J.; White, E.P.; Phillips, O.L.; Jørgensen, P.M.; Weiser, M.D.; Monteagudo Mendoza, A.; Núñez Vargas, P. Variation in above-ground forest biomass across broad climatic gradients. *Glob. Ecol. Biogeogr.* **2011**, *20*, 744–754. [CrossRef]
11. Babst, F.; Poulter, B.; Trouet, V.; Tan, K.; Neuwirth, B.; Wilson, R.; Carrer, M.; Grabner, M.; Tegel, W.; Levanic, T.; et al. Site- and species-specific responses of forest growth to climate across the European continent. *Glob. Ecol. Biogeogr.* **2013**, *22*, 706–717. [CrossRef]
12. Bouriaud, O.; Bréda, N.; Dupouey, J.-L.; Granier, A. Is ring width a reliable proxy for stem-biomass increment? A case study in European beech. *Can. J. For. Res.* **2005**, *35*, 2920–2933. [CrossRef]
13. Metsaranta, J.M.; Lieffers, V.J. Using dendrochronology to obtain annual data for modelling stand development: A supplement to permanent sample plots. *Forestry* **2009**, *82*, 163–173. [CrossRef]
14. Zweifel, R.; Eugster, W.; Etzold, S.; Dobbertin, M.; Buchmann, N.; Häsler, R. Link between continuous stem radius changes and net ecosystem productivity of a subalpine Norway spruce forest in the Swiss Alps. *New Phytol.* **2010**, *187*, 819–830. [CrossRef] [PubMed]
15. Metsaranta, J.M.; Kurz, W.A. Inter-annual variability of ecosystem production in boreal jack pine forests (1975-2004) estimated from tree-ring data using CBM-CFS3. *Ecol. Modell.* **2012**, *224*, 111–123. [CrossRef]
16. Esper, J.; Niederer, R.; Bebi, P.; Frank, D. Climate signal age effects-Evidence from young and old trees in the Swiss Engadin. *For. Ecol. Manag.* **2008**, *255*, 3783–3789. [CrossRef]
17. Frank, D.; Esper, J. Temperature reconstructions and comparisons with instrumental data from a tree-ring network for the European Alps. *Int. J. Climatol.* **2005**, *25*, 1437–1454. [CrossRef]
18. Büntgen, U.; Frank, D.C.; Kaczka, R.J.; Verstege, A.; Zwijacz-Kozica, T.; Esper, J. Growth responses to climate in a multi-species tree-ring network in the Western Carpathian Tatra Mountains, Poland and Slovakia. *Tree Physiol.* **2007**, *27*, 689–702. [CrossRef]
19. Friedrichs, D.A.; Trouet, V.; Büntgen, U.; Frank, D.C.; Esper, J.; Neuwirth, B.; Löffler, J. Species-specific climate sensitivity of tree growth in Central-West Germany. *Trees Struct. Funct.* **2009**, *23*, 729–739. [CrossRef]
20. Affolter, P.; Büntgen, U.; Esper, J.; Rigling, A.; Weber, P.; Luterbacher, J.; Frank, D. Inner Alpine conifer response to 20th century drought swings. *Eur. J. For. Res.* **2010**, *129*, 289–298. [CrossRef]
21. Briffa, K.R.; Osborn, T.J.; Schweingruber, F.H.; Jones, P.D.; Shiyatov, S.G.; Vaganov, E.A. Tree-ring width and density data around the Northern Hemisphere: Part 1, local and regional climate signals. *Holocene* **2002**, *12*, 737–757. [CrossRef]
22. Wettstein, J.J.; Littell, J.S.; Wallace, J.M.; Gedalof, Z. Coherent region-, species-, and frequency-dependent local climate signals in Northern hemisphere tree-ring widths. *J. Clim.* **2011**, *24*, 5998–6012. [CrossRef]

23. De Luis, M.; Čufar, K.; Di Filippo, A.; Novak, K.; Papadopoulos, A.; Piovesan, G.; Rathgeber, C.B.K.; Raventós, J.; Saz Sánchez, M.A.; Smith, K.T. Plasticity in dendroclimatic response across the distribution range of Aleppo pine (*Pinus halepensis*). *PLoS ONE* **2013**, *8*. [CrossRef] [PubMed]
24. Gazol, A.; Camarero, J.J.; Vicente-Serrano, S.M.; Sánchez-Salguero, R.; Gutiérrez, E.; de Luis, M.; Sangüesa-Barreda, G.; Novak, K.; Rozas, V.; Tíscar, P.A.; et al. Forest resilience to drought varies across biomes. *Glob. Chang. Biol.* **2018**, *24*, 2143–2158. [CrossRef] [PubMed]
25. Andreu-Hayles, L.; Gutiérrez, E.; Macias, M.; Ribas, M.; Bosch, O.; Camarero, J.J. Climate increases regional tree-growth variability in Iberian pine forests. *Glob. Chang. Biol.* **2007**, *13*, 804–815. [CrossRef]
26. Camarero, J.J.; Gazol, A.; Sangüesa-Barreda, G.; Cantero, A.; Sánchez-Salguero, R.; Sánchez-Miranda, A.; Granda, E.; Serra-Maluquer, X.; Ibáñez, R. Forest Growth Responses to Drought at Short- and Long-Term Scales in Spain: Squeezing the Stress Memory from Tree Rings. *Front. Ecol. Evol.* **2018**, *6*, 1–11. [CrossRef]
27. Linares, J.C.; Camarero, J.J.; Carreira, J.A. Competition modulates the adaptation capacity of forests to climatic stress: Insights from recent growth decline and death in relict stands of the Mediterranean fir Abies pinsapo. *J. Ecol.* **2010**, *98*, 592–603. [CrossRef]
28. Pacheco, A.; Camarero, J.J.; Ribas, M.; Gazol, A.; Gutierrez, E.; Carrer, M. Disentangling the climate-driven bimodal growth pattern in coastal and continental Mediterranean pine stands. *Sci. Total Environ.* **2018**, *615*, 1518–1526. [CrossRef] [PubMed]
29. Sánchez-Salguero, R.; Camarero, J.J.; Hevia, A.; Madrigal-González, J.; Linares, J.C.; Ballesteros-Canovas, J.A.; Sánchez-Miranda, A.; Alfaro-Sánchez, R.; Sangüesa-Barreda, G.; Galván, J.D.; et al. What drives growth of Scots pine in continental Mediterranean climates: Drought, low temperatures or both? *Agric. For. Meteorol.* **2015**, *206*, 151–162. [CrossRef]
30. Cavin, L.; Jump, A.S. Highest drought sensitivity and lowest resistance to growth suppression are found in the range core of the tree *Fagus sylvatica* L. not the equatorial range edge. *Glob. Chang. Biol.* **2016**, *23*, 1–18. [CrossRef] [PubMed]
31. Rozas, V.; Camarero, J.J.; Sangüesa-Barreda, G.; Souto, M.; García-González, I. Summer drought and ENSO-related cloudiness distinctly drive *Fagus sylvatica* growth near the species rear-edge in northern Spain. *Agric. For. Meteorol.* **2015**, *201*, 153–164. [CrossRef]
32. Legendre-Fixx, M.; Anderegg, L.D.L.; Ettinger, A.K.; HilleRisLambers, J. Site- and species-specific influences on sub-alpine conifer growth in Mt. Rainier National Park, USA. *Forests* **2017**, *9*, 1–16. [CrossRef]
33. Holmes, R.L. Computer-assisted quality control in tree-ring dating and measurement. *Tree-Ring Bull.* **1983**, *43*, 69–78. [CrossRef]
34. Cook, E.R. A Time Series Analysis Approach to Tree Ring Standardization. Ph.D. Thesis, The University of Arizona, Tucson, AZ, USA, August 1985.
35. Melvin, T.M.; Briffa, K.R. A "signal-free" approach to dendroclimatic standardisation. *Dendrochronologia* **2008**, *26*, 71–86. [CrossRef]
36. Carrer, M.; Urbinati, C. Age-Dependent Tree-Ring Growth Responses to Climate in *Larix decidua* and *Pinus cembra*. *Ecology* **2004**, *85*, 730–740. [CrossRef]
37. Serrano-Notivoli, R.; Beguería, S.; Saz Sánchez, M.A.; Longares Aladrén, L.A.; de Luis, M. SPREAD: A high-resolution daily gridded precipitation dataset for Spain. *Earth Syst. Sci. Data Discuss* **2017**, 1–33. [CrossRef]
38. Serrano-Notivoli, R.; de Luis, M.; Beguería, S. An R package for daily precipitation climate series reconstruction. *Environ. Model. Softw.* **2017**, *89*, 190–195. [CrossRef]
39. Larsson, L.A. *CooRecorder*; Cybis Elektronil and Data AB: Saltsjöbaden, Sweden, 2010.
40. Camarero, J.J.; Gazol, A.; Galván, J.D.; Sangüesa-Barreda, G.; Gutiérrez, E. Disparate effects of global-change drivers on mountain conifer forests: Warming-induced growth enhancement in young trees vs. CO2 fertilization in old trees from wet sites. *Glob. Chang. Biol.* **2015**, *21*, 738–749. [CrossRef] [PubMed]
41. Biondi, F.; Qeadan, F. Removing the tree-ring width biological trend using expected basal area increment. In *Fort Valley Experimental Forest-A Century of Research 1908–2008*; Olberding, S.D., Moore, M.M., Eds.; US Department of Agriculture, Forest Service, Rocky Mountain Research Station: Fort Collins, CO, USA, 2008.
42. De Martonne, E. Une nouvelle fonction climatologique: L'indice d'aridité. *La Meteorol.* **1926**, *2*, 449–458.
43. Bates, D.; Mächler, M.; Bolker, B.; Walker, S. Fitting Linear Mixed-Effects Models using lme4. *J. Stat. Softw.* **2015**, *67*. [CrossRef]

44. Burnham, K.P.; Anderson, D.R. *Model Selection and Multimodel Inference: A Practical Information-Theoretic Approach*, 2nd ed.; Springer: Berlin, Germany, 2002; ISBN 978-0-387-22456-5.
45. Peñuelas, J.; Sardans, J.; Filella, I.; Estiarte, M.; Llusià, J.; Ogaya, R.; Carnicer, J.; Bartrons, M.; Rivas-Ubach, A.; Grau, O.; et al. Impacts of global change on Mediterranean forests and their services. *Forests* **2017**, *8*, 1–37. [CrossRef]
46. Canadell, J.G.; Raupach, M.R. Managing forests for climate change mitigation. *Science* **2008**, *320*, 1456–1457. [CrossRef] [PubMed]
47. Esper, J.; Cook, E.R.; Schweingruber, F.H. Low-frequency signals in long tree-ring chronologies for reconstructing past temperature variability. *Science* **2002**, *295*, 2250–2253. [CrossRef] [PubMed]
48. Bowman, D.M.J.S.; Brienen, R.J.W.; Gloor, E.; Phillips, O.L.; Prior, L.D. Detecting trends in tree growth: Not so simple. *Trends Plant Sci.* **2013**, *18*, 11–17. [CrossRef] [PubMed]
49. D'Arrigo, R.; Wilson, R.; Liepert, B.; Cherubini, P. On the "Divergence Problem" in Northern Forests: A review of the tree-ring evidence and possible causes. *Glob. Planet. Chang.* **2008**, *60*, 289–305. [CrossRef]
50. Barbero, M.; Loisel, R.; Quézel, P.; Romane, F.; Richardson, D.M. Pines of the Mediterranean Basin. In *Ecology and Biogeography of Pinus*; Richardson, D.M., Ed.; Cambridge University Press: Cambridge, UK, 1998; ISBN 9780521789103.
51. Fernández-Pérez, L.; Villar-Salvador, P.; Martínez-Vilalta, J.; Toca, A.; Zavala, M.A. Distribution of pines in the Iberian Peninsula agrees with species differences in foliage frost tolerance, not with vulnerability to freezing-induced xylem embolism. *Tree Physiol.* **2018**, 507–516. [CrossRef] [PubMed]
52. Rouget, M.; Richardson, D.M.; Lavorel, S.; Vayreda, J.; Gracia, C.; Milton, S.J. Determinants of Distribution of Six Pinus Species in Catalonia, Spain. *J. Veg. Sci.* **2001**, *12*, 491–502. [CrossRef]
53. Zalloni, E.; de Luis, M.; Campelo, F.; Novak, K.; De Micco, V.; Di Filippo, A.; Vieira, J.; Nabais, C.; Rozas, V.; Battipaglia, G. Climatic signals from intra-annual density fluctuation frequency in mediterranean pines at a regional scale. *Front. Plant Sci.* **2016**, *7*. [CrossRef] [PubMed]
54. Novak, K.; de Luis, M.; Raventós, J.; Čufar, K. Climatic signals in tree-ring widths and wood structure of *Pinus halepensis* in contrasted environmental conditions. *Trees Struct. Funct.* **2013**, *27*, 927–936. [CrossRef]
55. Novak, K.; Čufar, K.; de Luis, M.; Saz Sánchez, M.A.; Raventós, J. Age, climate and intra-annual density fluctuations in *Pinus halepensis* in Spain. *IAWA J.* **2013**, *34*, 459–474. [CrossRef]
56. Pacheco, A.; Camarero, J.J.; Carrer, M. Linking wood anatomy and xylogenesis allows pinpointing of climate and drought influences on growth of coexisting conifers in continental Mediterranean climate. *Tree Physiol.* **2015**, *36*, 1–11. [CrossRef] [PubMed]
57. De Luis, M.; Novak, K.; Raventós, J.; Gričar, J.; Prislan, P.; Čufar, K. Cambial activity, wood formation and sapling survival of *Pinus halepensis* exposed to different irrigation regimes. *For. Ecol. Manag.* **2011**, *262*, 1630–1638. [CrossRef]
58. Voltas, J.; Chambel, M.R.; Prada, M.A.; Ferrio, J.P. Climate-related variability in carbon and oxygen stable isotopes among populations of Aleppo pine grown in common-garden tests. *Trees Struct. Funct.* **2008**, *22*, 759–769. [CrossRef]
59. Liphschitz, N.; Lev-Yadun, S.; Rosen, E.; Waisel, Y. The annual rhythm of activity of the lateral meristems (cambium and phellogen) in *Pinus halepensis* Mill. and *Pinus pinea* L. *IAWA Bull.* **1984**, *5*, 263–274. [CrossRef]
60. Prislan, P.; Gričar, J.; de Luis, M.; Novak, K.; Del Castillo, E.M.; Schmitt, U.; Koch, G.; Štrus, J.; Mrak, P.; Žnidarič, M.T.M.T.; et al. Annual Cambial Rhythm in *Pinus halepensis* and *Pinus sylvestris* as Indicator for Climate Adaptation. *Front. Plant Sci.* **2016**, *7*. [CrossRef] [PubMed]
61. Camarero, J.J.; Olano, J.M.; Parras, A. Plastic bimodal xylogenesis in conifers from continental Mediterranean climates. *New Phytol.* **2010**, *185*, 471–480. [CrossRef] [PubMed]
62. De Luis, M.; Novak, K.; Raventós, J.; Gričar, J.; Prislan, P.; Čufar, K. Climate factors promoting intra-annual density fluctuations in Aleppo pine (*Pinus halepensis*) from semiarid sites. *Dendrochronologia* **2011**, *29*, 163–169. [CrossRef]
63. Novak, K.; De Luis, M.; Gričar, J.; Prislan, P.; Merela, M.; Smith, K.T.; Čufar, K. Missing and Dark Rings Associated With Drought in *Pinus halepensis*. *IAWA J.* **2016**, *37*, 260274. [CrossRef]
64. Keenan, T.; Maria Serra, J.; Lloret, F.; Ninyerola, M.; Sabate, S. Predicting the future of forests in the Mediterranean under climate change, with niche- and process-based models: CO2 matters! *Glob. Chang. Biol.* **2011**, *17*, 565–579. [CrossRef]

65. Garzón, M.B.; Blazek, R.; Neteler, M.; Dios, R.S. De; Ollero, H.S.; Furlanello, C. Predicting habitat suitability with machine learning models: The potential area of *Pinus sylvestris* L. in the Iberian Peninsula. *Ecol. Modell.* **2006**, *197*, 383–393. [CrossRef]
66. Graumlich, L.J.; Brubaker, L.B.; Grier, C.C. Long-term trends in forest net primary productivity: Cascade Mountains, Washington. *Ecology* **1989**, *70*, 405–410. [CrossRef]
67. Babst, F.; Alexander, M.R.; Szejner, P.; Bouriaud, O.; Klesse, S.; Roden, J.; Ciais, P.; Poulter, B.; Frank, D.; Moore, D.J.P.; et al. A tree-ring perspective on the terrestrial carbon cycle. *Oecologia* **2014**, *176*, 307–322. [CrossRef] [PubMed]
68. Dye, A.; Plotkin, A.B.; Bishop, D.; Pederson, N.; Poulter, B.; Hessl, A. Comparing tree-ring and Permanent plot estimates of aboveground net primary production in three eastern U.S. forests. *Ecosphere* **2016**, *7*. [CrossRef]
69. Alexander, M.R.; Rollinson, C.R.; Babst, F.; Trouet, V.; Moore, D.J.P. Relative influences of multiple sources of uncertainty on cumulative and incremental tree-ring-derived aboveground biomass estimates. *Trees Struct. Funct.* **2018**, *32*, 265–276. [CrossRef]
70. Davis, S.C.; Hessl, A.E.; Scott, C.J.; Adams, M.B.; Thomas, R.B. Forest carbon sequestration changes in response to timber harvest. *For. Ecol. Manag.* **2009**, *258*, 2101–2109. [CrossRef]
71. Sass-Klaassen, U.G.W.; Fonti, P.; Cherubini, P.; Gričar, J.; Robert, E.M.R.; Steppe, K.; Bräuning, A. A tree-centered approach to assess impacts of extreme climatic events on forests. *Front. Plant Sci.* **2016**, *7*, 1069. [CrossRef] [PubMed]